

ELECTRIC QUADRUPOLE FOCUSING IN LINEAR ION ACCELERATORS

K. Blasche, R. Friehmelt, K. Kaspar, Ch. Schmelzer, U. Wolfangel
Institut für Angewandte Physik der Universität
Heidelberg, Germany

Abstract

The focusing in the first sections of heavy ion linear accelerators ($\beta=0.005$ to 0.04) may be achieved without the use of grids by employing electric quadrupole lenses. The focusing voltage required can be technically realized and would not exceed ± 15 kV in the Manchester heavy ion injector linac.

Using a low energy proton model (49 keV), the current yield and radial acceptance of the electric quadrupole focusing system have been studied. The experimental results are very interesting: the current yield is as high as 34% for the 24 drift-tube linac, and it rises to more than 60% when a buncher is used. A radial acceptance of 80 cm·mrad is measured.

To the first order, the theory is identical for both electric and magnetic fields. In the second order, the focusing is different, since the electric lenses modify the particle energy due to the fringing fields. Computational results concerning the field gradients and the radial acceptance including coupling effects are the bases for the choice of parameters of a heavy ion linac.

Introduction

The problem of focusing in heavy ion linacs has so far been solved by the use of grids fitted to the entrance of the drift tubes. This method, having a rather poor efficiency, was applied since the magnetic focusing fields in quadrupole lenses would be extremely high due to the low velocity of heavy ions.

For the small values of β , with which one is concerned in heavy ion linacs, electric quadrupole lenses do not call for very high supply voltages. In the case of the Berkeley Hilac prestripper, it is true that a 2 in. bore diameter requires an electrode voltage of ± 110 kV. On the other hand, such a large bore is not necessary. If a 3/4 in. bore were used, an electrode voltage of only ± 17.5 kV would be necessary.

Electric quadrupole lenses are

especially suitable for the twin-line structure employed in the heavy ion linacs in Manchester and Orsay. For example, such lenses have the advantage of no power consumption, and hence would do away with cumbersome cooling systems. In addition they are very light, and can be housed inside drift tubes with an outer diameter of only 10 cm.

Experiments carried out with a 5.5 MeV experimental proton linac in Kharkov (1955) indicated that electric quadrupole lenses compare favorably with the magnetic type (ref. 1). These investigations did not include such questions as the radial acceptance of the linac or the coupling effect between longitudinal and radial motion caused by the fringing fields of the electric quadrupole lenses.

In connection with design studies for a heavy ion linac, it was considered whether electric quadrupole lenses might be used in the first section of the linac. This stage is characterized by input velocities of the order $\beta = 0.005$ (0.01 MeV/nucleon) and output velocities of the order $\beta = 0.04$ (1 MeV/nucleon). The value of e/m , which is determined by the type of ion source available, may be as small as 0.04 for the heaviest ions. The usual rf structure for these β -values is the twin-line system (Sloan-Lawrence or Wideröe structure).

Within the framework of these design studies, experiments were performed with a low energy proton analog. This model has permitted detailed studies of particle dynamics in a short linac section with electric quadrupole focusing.

Electric Field Gradients and Radial Acceptance

As with all alternating gradient systems, focusing with quadrupole lenses will lead to stable operation only for certain values of the parameters. Phase oscillations make the problem more complicated. It is advisable, therefore, to consider the behaviour of the synchronous particle and subsequently to examine the general case.

Usually the necessary field gradients

are calculated by matrix multiplication (ref. 2). The product matrix representing a full repeat length is used to determine the quantity $\cos \mu_N$ and, hence, also the electric field gradients E' at the lower end of the stable region for $\cos \mu_N = 1$ (ref. 3):

$$E'_{\min}/kVcm^{-2} = 972 \cdot C(N,Q) \cdot \left(\frac{V/MV \cdot T \cdot f/Mcs^{-1} \cdot \beta \cdot \sin(-\varphi_s)}{e/m \cdot (L/cm)^3} \right)^{1/2}$$

where V is the accelerating voltage,
 T the transit time factor,
 f the frequency of the accelerating field,
 β the particle velocity,
 φ_s the synchronous phase,
 e/m the charge to mass ratio (proton: e/m = 1),
 L the rf cell length, and

C(N,Q) allows for different polarity groupings N and filling factors Q (the ratio between the length of the lens and the rf cell length), (fig. 1).

The corresponding magnetic field gradients are given by

$$B'/kGcm^{-1} = \frac{E'/kVcm^{-2}}{300 \cdot \beta}$$

For example, the field gradients required for the Manchester heavy ion linac with $V \cdot T = 0.1$ MV, $f = 25$ Mc/s, $\beta = 0.007$, $\varphi_s = -25^\circ$, $e/m = 0.125$, $L = 1/2 \cdot \beta \lambda$, $N = 2$, $Q = 0.5$ are

$$E' = 27.6 \text{ kV} \cdot \text{cm}^{-2} \quad \text{or} \quad B' = 13.2 \text{ kG} \cdot \text{cm}^{-1}$$

With a bore diameter of 2 cm, the voltage required on the electrodes would be 13.8 kV. If magnetic quadrupole lenses were used, the magnetic field at the pole tips would be 13.2 kG. Fig. 2 shows the stable region for the Manchester linac and the radial acceptance, $A_x = A_y$, for the two transverse directions and their common area, A_s .

The field gradients decrease with increasing particle velocity, and may be chosen, for instance, according to $\cos \mu_N = \text{constant}$. In this case, the radial acceptance calculated for the first rf cell length is in good agreement with the radial acceptance determined by computing the particle orbits. There are other possibilities available for choosing the field gradients. In the proton model, the field gradients are constant for the first 14 drift tubes and again for the following 10 drift tubes (fig. 3). Because the field gradients are not reduced according to $\cos \mu_N = \text{constant}$, the radial acceptance determined by computing the particle orbits is larger than the accep-

tance evaluated for the first rf cell length (fig. 4).

In any resonant accelerator, there exist coupling forces between the longitudinal and the radial motion. These forces have not been taken into account when the radial acceptance has been calculated for the synchronous particle. The fringing fields of the electric quadrupole lenses alternately accelerate and decelerate the particles, and thus increase the coupling effect in the case of electric quadrupole focusing. From fig. 5 it is seen that there are different radial acceptances for particles with different phase angles at injection. These radial acceptances are in general smaller than that for the synchronous particle (fig. 4b).

The Low Energy Proton Model

Important properties of an electric quadrupole system may be investigated by using a proton beam to simulate the heavy ion beam. The requirements for the proton analog are that the electromagnetic fields and the kinetic energies of the protons be reduced by the value of e/m for heavy ions, which is assumed to be 0.02. Space and time parameters, beam dynamics, and applied frequency remain full-scale. A practical advantage of the analog system is that the conditions impose only modest demands on high voltage supplies and rf power equipment (ref. 4).

The accelerator is a machine of the Sloan-Lawrence type, employing a symmetric transmission line (fig. 6). Its basic characteristics are as follows:

frequency of accelerating field.	15 Mc/s
length of accelerating structure	2 m
number of drift tubes.....	24
length of first drift tube.....	3.64 cm
length of last drift tube.....	7.61 cm
lengths of accelerating gaps	
gap number 1 - 14.....	1.5 cm
gap number 15 - 25.....	2.5 cm
aperture of drift tubes and	
quadrupole lenses.....	3.0 cm
outer diameter of drift tubes...	8.0 cm
rf peak voltage.....	2 kV
synchronous phase.....	-28.6°
injection velocity, β_i	0.005
final velocity, β_f	0.01
accelerating mode.....	$1/2 \cdot \beta \lambda$

Fig. 7 shows a drift tube with an electric quadrupole lens. Although there is only a 3 mm space between the drift-tube shell and the electrodes of the quadrupole lens, a voltage of more than 20 kV can be applied to the electrodes.

The ion source is a standard rf

source that produces a 1 mA beam with about 70% protons and 30% H_2^+ and H_3^+ ions. Between the ion source and the accelerator a buncher is installed. The beam current injected into the accelerator is of the order of a few hundred microamperes.

The beam-detection equipment consists of several Faraday cages, a mobile one at the input end, another one at the output of the linac, and a special one with a wide pass band of about 300 Mc/s. An emittance measuring device can be placed at the input or output of the accelerator (ref. 5). The energy spectrum is studied with a magnetic 45° -spectrometer. Measurements of the radial acceptance have been carried out by using a pair of adjustable slits collimating the beam.

Experimental Results

One important quantity describing the focusing properties of any system is the current yield, which is usually measured by comparing input and output beam currents. The current yield can be as high as 34%, and rises to more than 60% when a buncher is used. With no focusing voltage applied to the electrodes of the quadrupole lenses, only 15% of the injected beam current is measured at the exit.

Let us consider these figures in more detail. The output current is limited principally by the phase acceptance because only about 65% of the injected protons are trapped in the phase stable region around $\psi_s = -28.6^\circ$. The remaining 35% are deflected by the strong focusing fields in the electric quadrupole lenses, and do not appear in the output current if the focusing voltage is adjusted for optimal current yield. Fig. 8 shows two energy spectra recorded at the exit of the accelerator. When little or no focusing voltage is applied, the beam contains only a small fraction of 49 keV protons, whereas there is a large intensity at the injection energy of 11.7 keV. With optimal focusing voltage, however, the 49 keV proton peak increases strongly, whereas the low energy particles are entirely suppressed.

The current yield does not depend only on the qualities of the focusing system but also on the emittance of the injected beam. Fig. 9 shows the measured emittance of the beam at the input and at the output of the accelerator. The injected beam has a diameter of 2 cm, whereas the accelerated beam is focused to a diameter of 0.5 cm. Due to the acceleration, the emittance of the beam at the exit is reduced by a factor of two. Fig. 10 a shows a photograph of the

image that the proton beam produces on a screen after being accelerated. The size of the beam cross section, which depends on the applied focusing voltage, is about 4 x 8 mm. The irregular shape of the beam cross section might be due to the coupling effect between longitudinal and radial motions. Aberrations of the quadrupole lenses are probably not the source of the irregular shape, since the distortion does not appear when the beam passes through the quadrupole lenses without being accelerated (fig. 10 b).

In order to determine the radial acceptance, the transmission of the beam was measured systematically across the $x - x'$ plane and the acceptance limits were arbitrarily set at a transmission of 5%. The radial acceptance for both transverse directions is shown in fig. 11. These measurements indicate a rather good agreement with the radial acceptance shown in fig. 5.

We have discussed the influence of the coupling effects on the radial motion, but not yet the effect of the radial motion on the phase motion. Due to the fringing fields of the electric quadrupole lenses, the particles are accelerated and decelerated according to their radial distance (fig. 12). Nevertheless, the energy spread does not exceed $\pm 2\%$ (fig. 8), and the phase damping results in short particle bunches (fig. 13). The efficiency of the electric quadrupole focusing system is shown by the fact that no particle bunches are observed on the screen of a sampling oscilloscope when the focusing voltage is switched off.

References

1. L. I. Bolotin et al., "Strong Focusing in Linear Accelerators", CERN-Symposium, 644 (1959).
2. L. Smith, R. L. Gluckstern, "Focusing in Linear Ion Accelerators", Rev. Sci. Instr. 26, 220 (1955).
3. R. Friehmelt, "Dimensionierung der Quadrupolfokussierung in einem Schwerionen-Linearbeschleuniger", UNILAC-Bericht Nr. 5-67, Heidelberg (1967).
4. K. Blasche, "Elektrostatische Quadrupolfokussierung in Linearbeschleunigern für schwere Ionen", UNILAC-Bericht Nr. 6-67, Heidelberg (1967).
5. K. Kaspar, "Untersuchungen zur Messung der Emittanz von Ionenstrahlen", UNILAC-Bericht Nr. 4-67 int., Heidelberg (1967).

This work was supported by the Federal Ministry for Scientific Research.

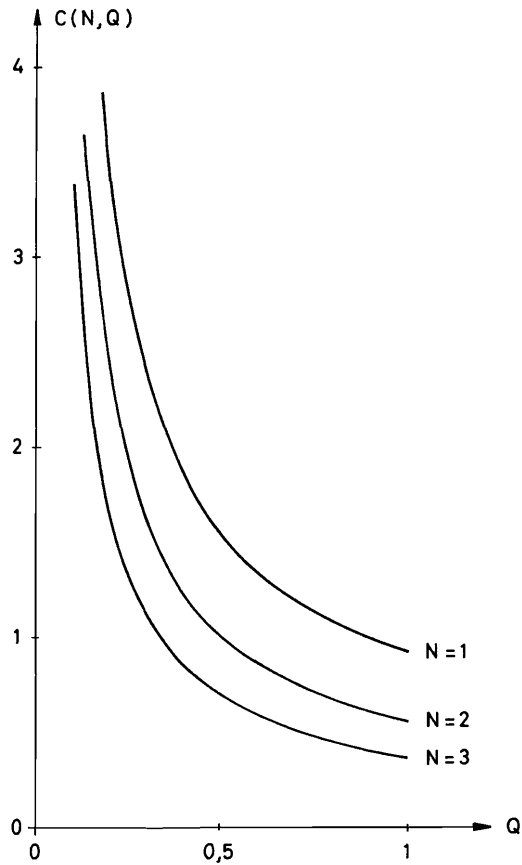


Fig. 1. Diagram of the function $C(N, Q)$.

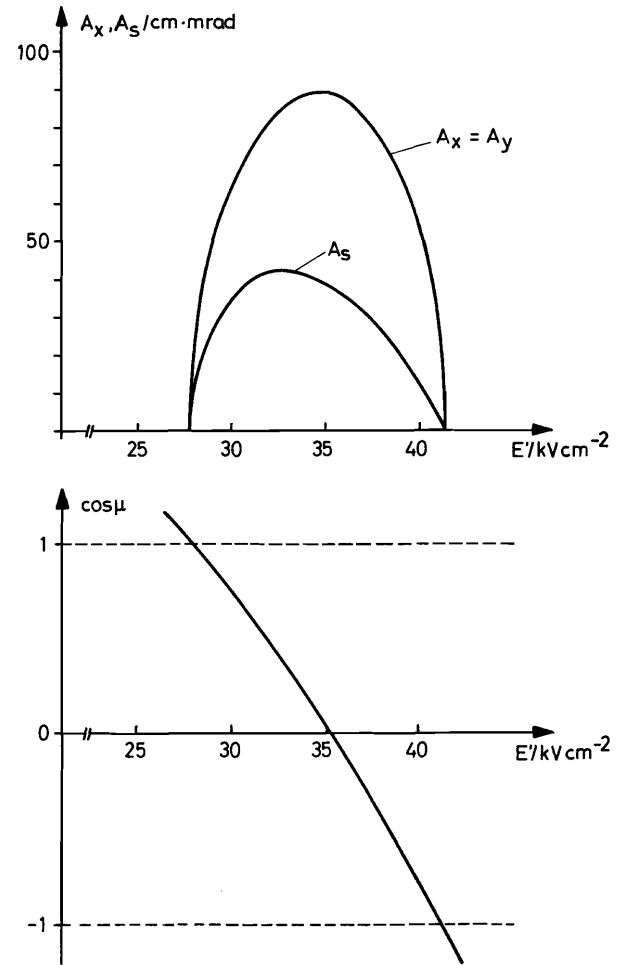


Fig. 2. Radial acceptance and stable region for the Manchester linac.

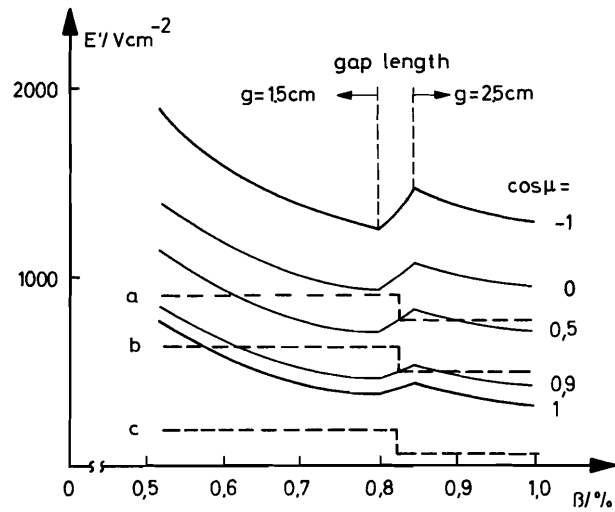


Fig. 3. Stable region for the proton model with field gradients applied for experiments ($N=2$).

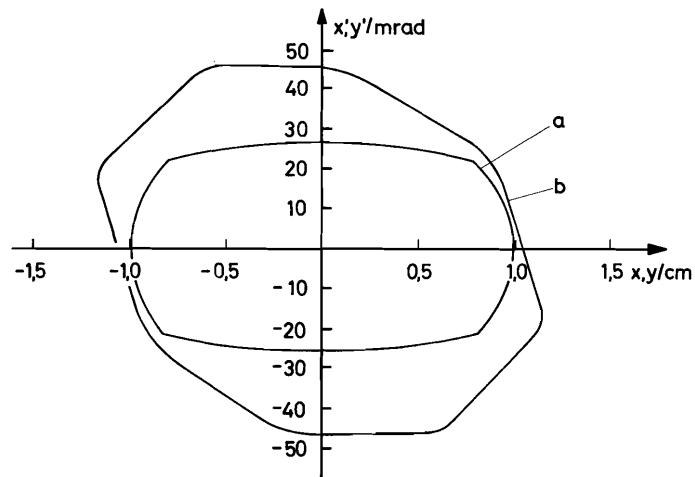


Fig. 4. Radial acceptance A_S of the proton model. Coupling effects are neglected.
 a. calculation for the first rf cell length,
 b. trajectory calculations.

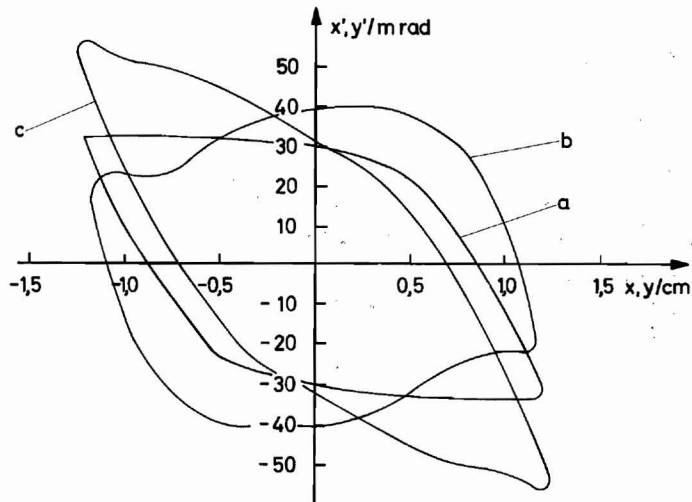


Fig. 5. Radial acceptance A_s of the proton model for particles with different phase angles at injection. Coupling effects are included. Injection phases = :
 a. $=0^\circ$, b. $=+30^\circ$, c. $=-30^\circ$

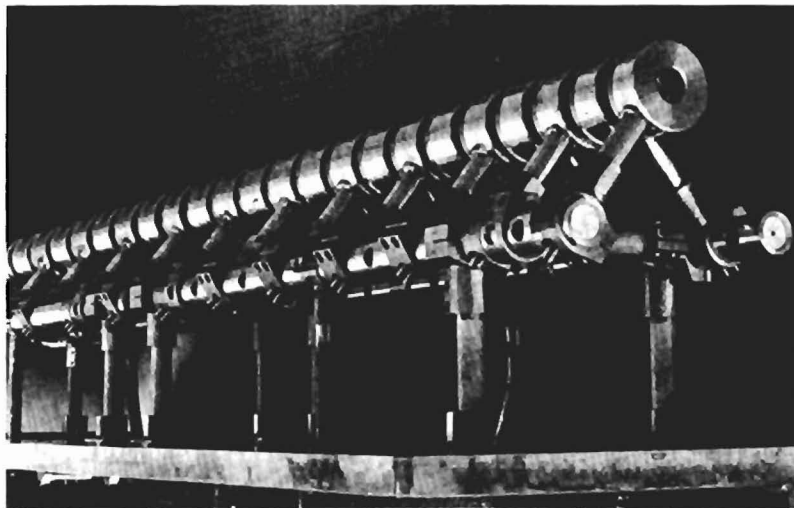


Fig. 6. Accelerating structure of the proton model.

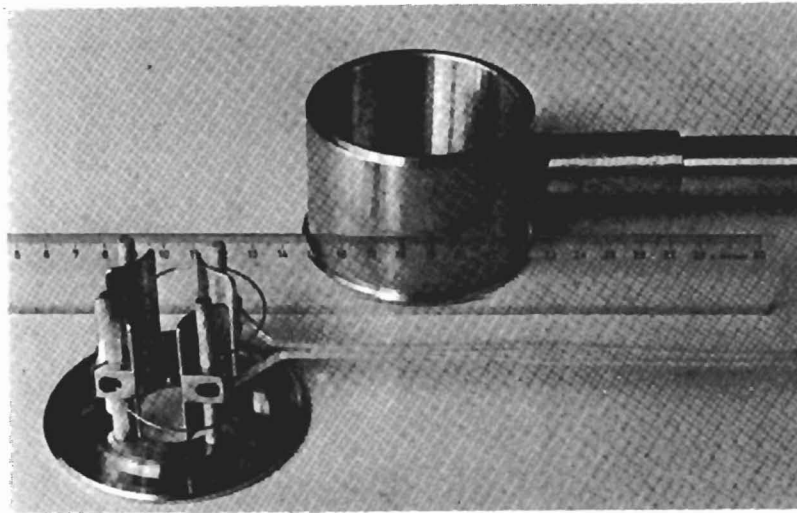


Fig. 7. Drift tube with electric quadrupole lens.

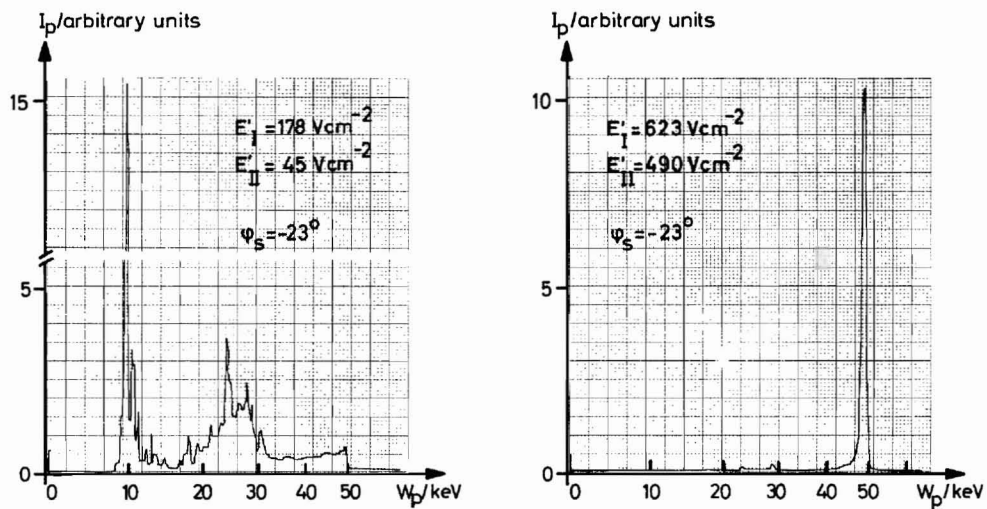


Fig. 8. Energy spectra of the proton beam. Field gradients are constant in the first 14 quadrupole lenses (E'_I) and again in the following 10 lenses (E'_{II}).

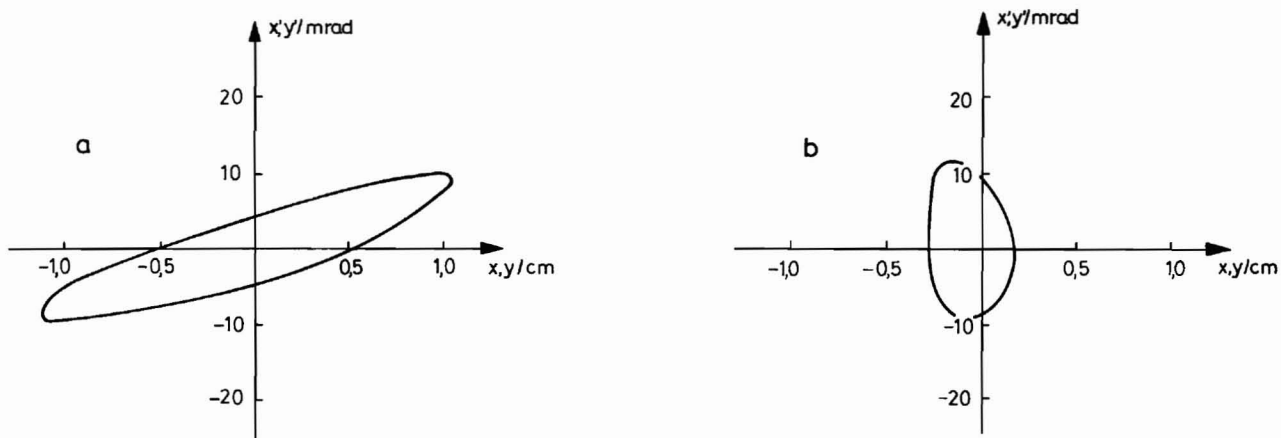


Fig. 9. Measured emittance of the proton beam. Field gradients are $E_I^z = 800 \text{ V cm}^{-2}$ and $E_{II}^z = 655 \text{ V cm}^{-2}$. a. injection, b. output end.

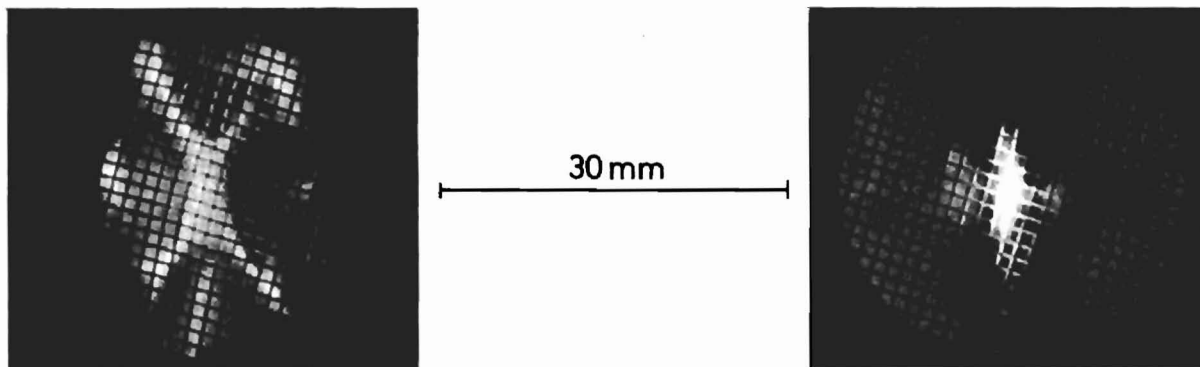


Fig. 10. Image of proton beam at the output end.
 a. rf acceleration, $\theta_s = -28^\circ$, $E_I^z = 935 \text{ V} \cdot \text{cm}^{-2}$, $E_{II}^z = 755 \text{ V} \cdot \text{cm}^{-2}$.
 b. no rf acceleration, $E_I^z = E_{II}^z = 260 \text{ V} \cdot \text{cm}^{-2}$.

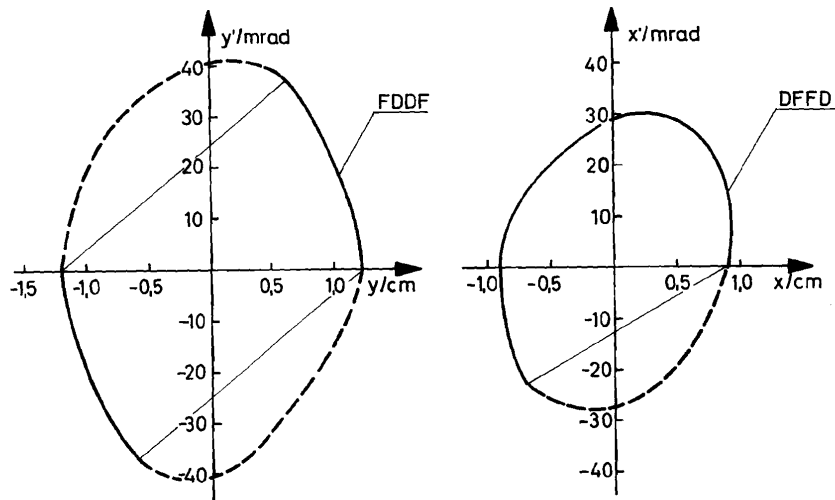


Fig. 11. Radial acceptance of the proton model. $E_{iI} = 890 \text{ V}\cdot\text{cm}^{-2}$, $E_{iII} = 755 \text{ V}\cdot\text{cm}^{-2}$, $s = -28^\circ$.
 — limit of the radial acceptance (5% transmission),
 - - - extrapolated.

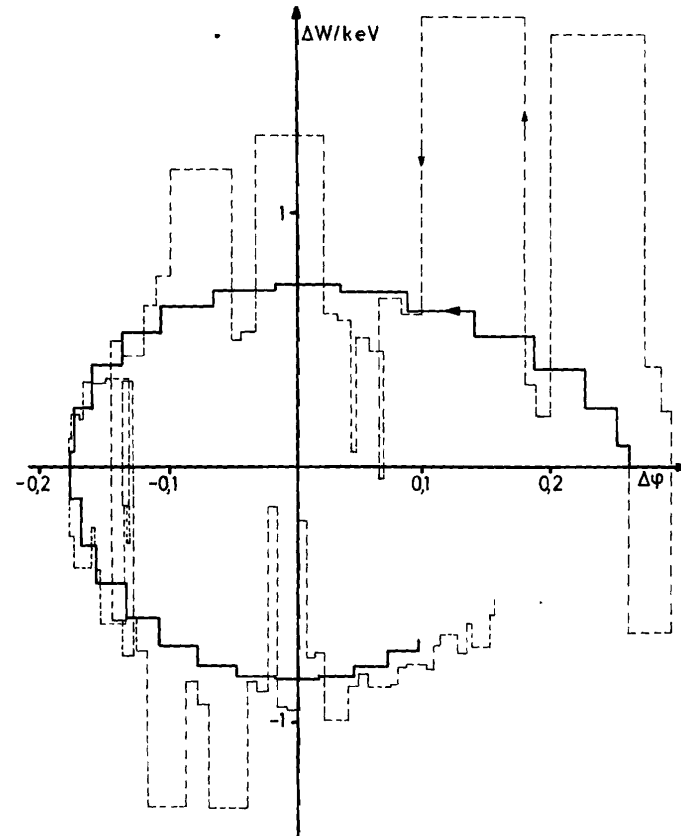


Fig. 12. Modification of the phase motion in the proton model by the radial oscillations.
 — without coupling effects,
 - - - coupling effects are included.

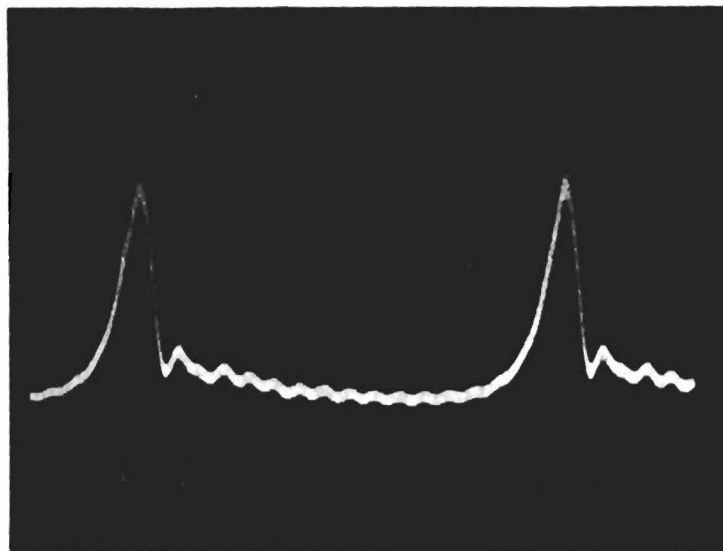


Fig.13. Particle bunches at the exit of the proton model recorded by a 300 Mc/s broad-band Faraday cage and a sampling oscilloscope.